Developing a Snow Algae Model to Reconstruct Blooming at the Global Scale Using a Land Surface Model

Yukihiko Onuma[1], Kei Yoshimura[2], and Nozomu Takeuchi[3]

[1]The University of Tokyo
[2]University of Tokyo
[3]Chiba University

March 25, 2021

Abstract

Snow algae are found from spring to summer on snowfields and glaciers throughout the world. Their blooming darkens snow surfaces, reducing snow surface albedo and accelerating melting. Uncertainties remain, however, regarding the blooming season and global distribution of these algae. To reproduce snow algal bloom temporal and spatial variability, we improved an existing snow algae model using a land surface model calibrated with a global atmospheric reanalysis dataset. Snowfall and daylight length data for selected model locations were also incorporated. To evaluate its performance, we used *in situ* observational data from 15 polar to alpine area sites. The improvements made in this study allowed the reconstruction of detailed snow algal blooming reports from various locations worldwide, and the results suggested that the major factors affecting the appearance of snow algal blooming were the snow melting period duration and algal growth interruption by new snow cover. We then incorporated the updated snow algae model into a land surface model and performed a global simulation. In this case, our simulation suggested that red snow could appear on snowfields during the melting season but only in the absence of frequent new snow falls, and if the snow cover persists long enough to allow prolonged algal growth.

Hosted file

`onuma_20210322_jgr_si.docx` available at https://authorea.com/users/539614/articles/599962-developing-a-snow-algae-model-to-reconstruct-blooming-at-the-global-scale-using-a-land-surface-model

Developing a Snow Algae Model to Reconstruct Blooming at the Global Scale Using a Land Surface Model

Y. Onuma[1], K. Yoshimura[1], and N. Takeuchi[2]

[1]Institute of Industrial Science, University of Tokyo, Chiba, 277-8574, Japan

[2]Graduate School of Science, Chiba University, Chiba, 263-8522, Japan

Corresponding author: Yukihiko Onuma (onuma@iis.u-tokyo.ac.jp)

Key Points:

- Red snow phenomena caused by snow algal blooming happen on snowfields and glaciers worldwide
- Red snow algae model was updated with new observational data from 15 snowfields and incorporated into a land surface model
- Revised model simulations achieved good agreement with red snow observations at snowfields worldwide, from polar to mid-latitudes

Abstract

Snow algae are found from spring to summer on snowfields and glaciers throughout the world. Their blooming darkens snow surfaces, reducing snow surface albedo and accelerating melting. Uncertainties remain, however, regarding the blooming season and global distribution of these algae. To reproduce snow algal bloom temporal and spatial variability, we improved an existing snow algae model using a land surface model calibrated with a global atmospheric reanalysis dataset. Snowfall and daylight length data for selected model locations were also incorporated. To evaluate its performance, we used *in situ* observational data from 15 polar to alpine area sites. The improvements made in this study allowed the reconstruction of detailed snow algal blooming reports from various locations worldwide, and the results suggested that the major factors affecting the appearance of snow algal blooming were the snow melting period duration and algal growth interruption by new snow cover. We then incorporated the updated snow algae model into a land surface model and performed a global simulation. In this case, our simulation suggested that red snow could appear on snowfields during the melting season but only in the absence of frequent new snow falls, and if the snow cover persists long enough to allow prolonged algal growth.

1 Introduction

Snow algae are photosynthetic microbes growing on snow and ice and are common globally in snowfields and glaciers. Snow algal blooms occur on thawing snow surfaces and change the color of the snow to red, orange, or green (Hoham and Remias, 2020). In particular, the red snow phenomenon, which is caused by blooms of *Sanguina* (*S.*) *nivaloides* (renamed from *Chlamydomonas nivalis* by Procházková et al., 2019) and *Chloromonas* sp., have been reported throughout spring and summer seasons worldwide (Thomas and Duval, 1995; Painter et al., 2001; Novis, 2002; Takeuchi and Kohshima, 2004; Takeuchi et al., 2006a; Stibal et al., 2007; Fujii et al., 2010; Spijkerman et al., 2012; Lutz et al., 2014, 2015, 2016; Hisakawa et al., 2015; Cepák et al., 2016; Remias et al., 2016; Tanaka, 2016; Tanaka et al., 2016; Ganey et al., 2017; Huovinen et al., 2018; Moestrup et al., 2018; Segawa et al., 2018; Onuma et al., 2018; Procházková et al., 2019; Zawierucha and Shain, 2019; Vimercati et al., 2019) (Fig. 1). The conditions required for snow algal growth include the availability of liquid water, solar radiation, and nutrients (Hoham and Remias, 2020). Previous studies have suggested that snow algal abundance can change significantly over time, due to their growth, accumulation, and cell losses during the snow-melting season (Müller et al., 2001; Takeuchi, 2013; Onuma et al., 2016, 2018). However, it is unclear exactly when and where the red snow phenomenon appears in snowfields and glaciers worldwide.

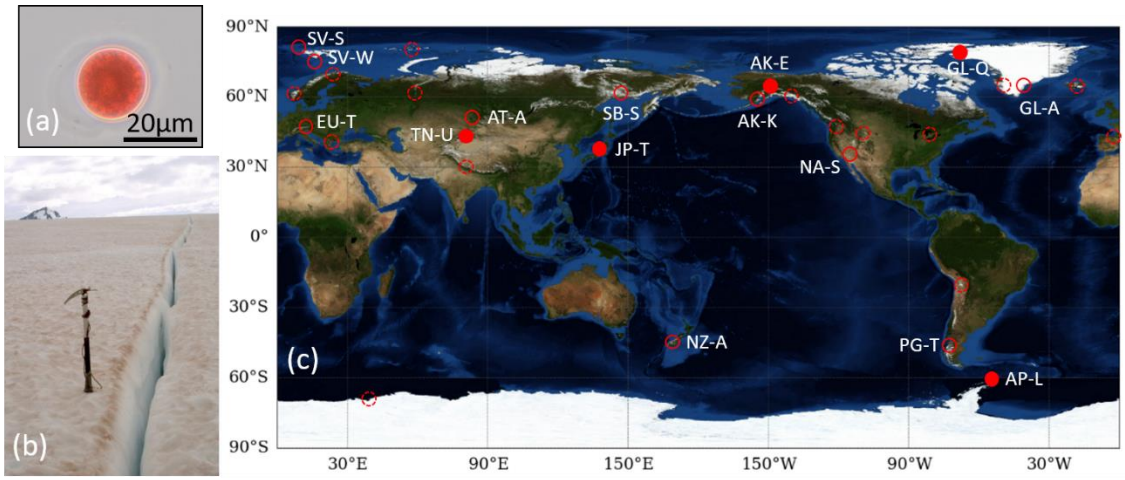

Figure 1 a red snow algae; **b** the red snow phenomenon on an Alaskan snowfield; **c** previously reported distribution of the red snow phenomena on snowfields and glaciers worldwide. Solid, open, and open-dotted marks indicate seasonal data validation sites, one-day data validation sites, and no applicable sites in this study, respectively. Only validation sites where red snow algal abundance was quantified by the cell count method were used. Site names correspond to those in Table 1

To reproduce snow algal growth and evaluate its impact on snow melting, a numerical equation, the "snow algae model," was recently proposed. Field observations in a Greenlandic glacier showed that snow algal abundance exponentially increased with snow melting, provided there was no intervening snowfall, reaching the carrying capacity of the snowpack in late summer (Onuma et al., 2018). An increase in snow algal abundance with snow melting has also been reported for Alaska and Japan (Takeuchi, 2013; Onuma et al., 2016). Based on these field observations, Onuma et al. (2018) established a numerical model for snow algal growth. The model was able to simulate the exponential growth of *S. nivaloides* using biological parameters (initial cell concentration, growth rate, and carrying capacity) and the duration of snow melting. The snow algae model was then incorporated into a physically based snow albedo model (Aoki et al., 2011; Onuma et al., 2020), which calculated the surface albedo of snow containing black carbon, mineral dust, and snow algae.

Many studies have suggested that algal abundance can be affected by atmospheric conditions, as well as by the physical and chemical conditions of snow, such as snow melting, snowfall, solar radiation, and nutrient availability (Stibal et al., 2007; Takeuchi, 2013; Lutz et al., 2014; Onuma et al., 2016, 2018; Hoham and Remias, 2020). The snow algae model did not include such effects on algal growth, however, and it was evident that variables such as daylight length and snowfall events in particular, which affect algal photosynthesis and vary across global locations, should be considered if the model was to be applied to other snowfield or glacier sites. Although there have been a number of studies on snow algae worldwide, most lack the *in situ* data for meteorological conditions and snow physics—including air temperature, solar radiation, precipitation, snow depth in water equivalent, and snow temperature—which are required to evaluate the snow algae model. This suggested that a dataset of snow physics and meteorological conditions obtained from a land surface model and global reanalysis data may be useful for

evaluating the snow algae model using snow algal data in published papers as well as for simulating snow algal growth globally.

A number of land surface models, which can be driven using reanalysis data, have been proposed to simulate temporal and spatial changes in snow properties on a global scale. For example, CLM (Lawrence et al., 2019), ORCHIDEE (Krinner et al., 2005), ISBA (Decharme et al., 2016), and MATSIRO (Takata et al., 2003; Nitta et al., 2014; 2017) have been established as land surface models incorporated into climate models to represent physical land processes. These models can calculate temporal and spatial changes in the snow water equivalent, snow temperature, water runoff, evaporation, and sublimation globally. In addition, a simulation with a land surface model can be conducted independently, using atmospheric conditions near the land surface as the input data. Such a simulation is termed an offline land simulation. Global atmospheric reanalysis data are generally used as atmospheric conditions for offline land simulations, which allows temporal and spatial changes in land physical properties to be reproduced without model bias that may derive from atmospheric conditions.

In this study, we first improved the snow algae model using *in situ* snow algal abundance data, as reported from 15 locations worldwide, and the physical and meteorological snow conditions for these locations, as obtained from a land surface model. We incorporated the effect of snowfall and daylight length into the snow algal model established by Onuma et al. (2018) and then conducted offline land simulations at the study sites using various atmospheric conditions and biological parameters. Finally, we performed a global simulation of the land surface model, including the snow algae model, using atmospheric reanalysis data sets to investigate seasonal and geographical variations in snow algal blooms worldwide.

2 Model description and experimental design

2.1 Snow algae model

We used a snow algae model to calculate temporal changes in the abundance of snow algae across various snowfields. Temporal changes in the abundance of *S. nivaloides* on surface snow can be expressed using a differential logistic growth equation. The population density and growth period of the microbes were calculated as shown in Eqs (1) and (2) (Onuma et al., 2018):

$$\frac{dX}{dGP_t^M} = \mu X_0 \left(1 - \frac{X_0}{K}\right), \text{ and} \tag{1}$$

$$\begin{cases} GP_t^M = GP_{t-1}^M + 1 \ (T_{sn1} \geq 273.15[K]) \\ GP_t^M = GP_{t-1}^M \ (T_{sn1} < 273.15[K]) \end{cases}, \tag{2}$$

where X and X_0 represent population densities of microbes at growth periods $GP^M{}_t$ and $GP^M{}_{t0}$, respectively, and μ indicates the hourly microbe growth rate. K denotes the snow surface algae carrying capacity, and $GP^M{}_{t0}$ represents the day that algae first appear on the snow surface. $GP^M{}_t$ represents the cumulative hours when the snow surface temperature, T_{sn1}, is above 0 ℃ (as algal growth only occurs on the melting snow surface). Although algal cells observed in the red snow surface are often in the cyst stage (e.g. Onuma et al., 2018)—when their populations do not

actively increase—the model assumes algal growth on the snow surface, including the condensation of algal cells grown at the subsurface, with snow melt.

In this study, we improved this model, which may include growth and / or condensation of the algal cells, to broadly reconstruct *in situ* observations of algal cell abundance reported for snow surfaces worldwide. To calculate temporal changes in the abundance of red snow algae on surface snow at various locations, we added the effects of snowfall and daylight length into the original snow algae model proposed by Onuma et al. (2018).

Onuma et al. (2016) reported that the abundance of a snow alga *Chloromonas* (*C.*) *nivalis* on a snowpack in Japan decreased when there were occasional snowfalls in spring; however, the snow algae model was not able to simulate such a decrease because it assumed a monotonic algal abundance increase. Because the snow algae model could calculate temporal changes in algal cell concentration in a surface snow layer to a depth of 2 cm, the accumulation of new snow above the algal layer should result in a decline in algal cell concentration. In this study, we updated the snow algae model to quantify the effect of snowfall on algal abundance in the top 2 cm layer of surface snow.

Daylight length is another metric with the potential of affecting algal growth because snow algae grow photosynthetically. A previous study reported that snow algal blooms first appeared under light conditions with a penetration of 0.1 % of the surface radiation (Curl et al., 1972), suggesting that snow algae on snow surfaces can grow during daylight but not during the night. Therefore, we assumed that snow algae grow in sunlight and incorporated a day–night cycle effect on snow algal growth into the snow algae model, as shown in Eq. (3):

$$\begin{cases} GP_t^{MR} = GP_{t-1}^{MR} + 1 \ (T_{sn1} \geq 273.15\ [K]\ and\ Sw > 0\ [Wm^{-2}]) \\ GP_t^{MR} = GP_{t-1}^{MR} \ (T_{sn1} < 273.15\ [K]\ or\ Sw = 0\ [Wm^{-2}]) \end{cases}, \quad (3)$$

where $GP^{MR}{}_t$ is defined as the cumulative hours of snow melting under daylight conditions, which can increase when the snow surface temperature, T_{sn1}, and downward shortwave radiation, Sw, are above 273.15 K and 0 W m^{-2}, respectively, at t.

We added two further equations to the calculation of snow algal growth, to quantify the effect of snowfall on snow algal abundance, as shown in Eqs (4)–(6):

$$X'^{MRF}_{t-1} = X^{MRF}_{t-1}\left(1 - \frac{P_{sn} * 3600 * 1000}{20 * D_{sn}}\right), \quad (4)$$

$$GP'^{MRF}_{t-1} = \frac{log_e\left(\frac{b}{a}\right)}{-\mu},\ a = \frac{(K - X_0)}{X_0},\ b = \frac{K}{X'^{MRF}_{t-1}} - 1, \text{ and} \quad (5)$$

$$\begin{cases} GP_t^{MRF} = GP'^{MRF}_{t-1} + 1 \ (T_{sn1} \geq 273.15\ [K]\ and\ Sw > 0\ [Wm^{-2}]) \\ GP_t^{MRF} = GP'^{MRF}_{t-1} \ (T_{sn1} < 273.15\ [K]\ or\ Sw = 0\ [Wm^{-2}]) \end{cases}, \quad (6)$$

where $X^{MRF}{}_t$ indicates algal cell concentration during the growth period ($GP^{MRF}{}_t$), including the effects of snow melting, daylight length, and snowfall. $X^{MRF}{}_t$ decreases based on the snowfall rate P_{sn} (mm s^{-1}), when snowfall occurs. If the new snow cover, which is calculated using P_{sn} and snow density D_{sn} (kg m^{-3}), exceeds 20 mm in 1 h, $X'^{MRF}{}_t$ is reset to X_0. In this study, D_{sn} was assumed to be 300 kg m^{-3}, which is generally used for this parameter in land surface models.

152 $GP^{'MRF}_t$ in Eq. (5) has been changed from Eq. (1) and represents the growth period at $X^{'MRF}_t$. In
153 this study, GP^{MRF}_t was used as the GP^{M}_t in Eq. (1), to calculate hourly algal cell concentrations.

154 An overview of the updated snow algae model can be seen in Fig. 2. In the model, initial
155 cell concentration, X_0, becomes established at the first snow appearance, and then the cell
156 concentration increases with the duration of snow melting under daylight conditions before
157 decreasing when new snowfall covers the surface. As the model could not consider the migration
158 of motile algal cells in a snowpack, algal cell concentrations reduced by snowfall were not
159 conserved in the model snow layers and did not increase again until there was further snow
160 melting under daylight conditions. The modeled algal cell concentrations reverted to zero once
161 the snowpack disappeared.

162

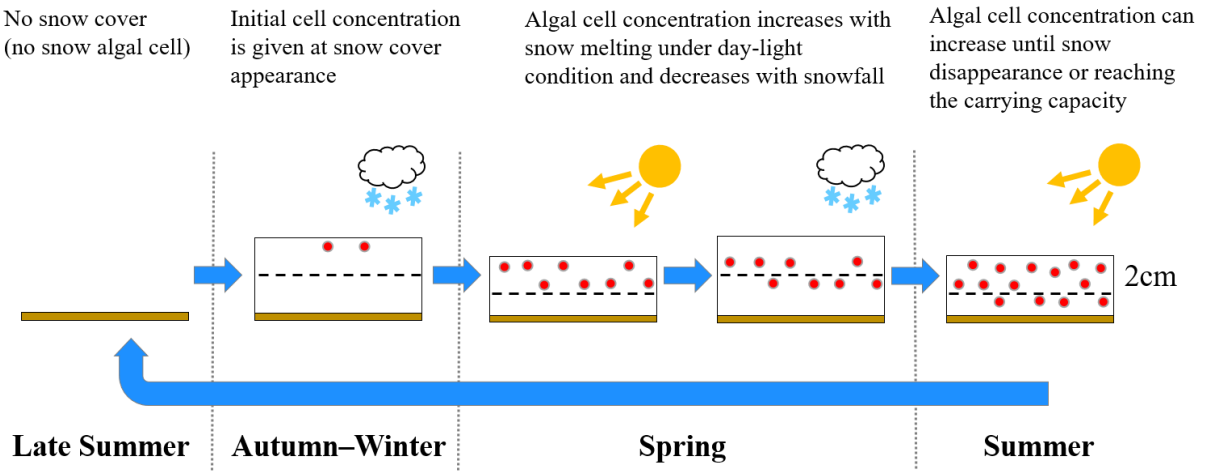

163

164 **Figure 2**. Concept supporting the updated snow algae model in this study. Dashed line indicates
165 the snow surface (top 2 cm) where snow algal cell can increase in snow algae model

166

167 2.2. Using *in situ* data for snow algal abundance to validate the snow algae model

168 In this study, we used temporal changes in algal cell abundance observed *in situ* at 15
169 locations as model validation data. An overview of the validation sites located in polar and alpine
170 regions—six sites representing sites used in previous studies, and nine representing those
171 observed specifically for this work—can be seen in Fig. 1**c** and Table 1.
172

Table 1. Maximum algal cell concentrations reported for red algal blooms from various snow fields

Site names	Study sites (Region)	Location	Elevation [m]	Red snow algal species	Maximum algal cell concentration [cells m^{-2}]	References
SV-S	Spitsbergen Island (North West Svalbard)	79.01N 12.48E	350	*Chloromonas sp.*	2.0×10^8	Lutz et al., 2015
GL-Q	Qaanaaq Area (North West Greenland)	77.5N 69.17W	944	*S. nivaloides*	3.5×10^7	Onuma et al., 2018
SV-W	Wedel Jarlsberg Land (South West Svalbard)	77.04N 15.14E	100	*S. nivaloides*	5.9×10^9	Stibal et al., 2007
GL-A	Ammassalik Island (South East Greenland)	65.6N 37.8W	150	*S. nivaloides*	1.8×10^8	Lutz et al., 2014
AK-E	Eastern Alaska Mountains (Alaska, USA)	64N 146W	1680	*S. nivaloides*	5.1×10^7	Takeuchi, 2013
SB-S	Suntar-Khayata Mountains (Siberia, Russia)	62.5N 141E	2509	*Chloromonas sp.*	1.8×10^8	Tanaka et al., 2016
AK-K	Kenai Mountains (Alaska, USA)	60N 150W	1100	*S. nivaloides*	6.7×10^9	Takeuchi et al., 2006b
AT-A	Altai Mountains (Altai, Russia)	49.51N 86.33E	3130	*Chloromonas sp.*	2.2×10^6	Takeuchi et al., 2006a
EU-T	Tyrol Mountains (Austria, Europe)	46.55N 10.55E	2975	*S. nivaloides*	5.0×10^8	Remias et al., 2016
TN-U	Urumqi Glacier (Tienshan, China)	43.06N 86.49E	4090	*Chloromonas sp.*	1.3×10^6	Tanaka, 2016
NA-S	Sierra Nevada Mountains (California, North America)	37.55N 119.55W	3425	*S. nivaloides*	1.3×10^7	Painter et al., 2001
JP-T	Tateyama Mountains (Japan)	36.34N 137.36E	2300	*S. nivaloides*	1.1×10^8	This study
NZ-A	Arthur's Pass Mountains (New Zealand)	42.89S 171.53E	1967	*Chlainomonas kolii*	1.2×10^7	Novis et al., 2002
PG-T	Tyndall Glacier (Southern Patagonia Ice fields, Chile)	51.15S 73.15W	1100	*Chloromonas sp.*	6.0×10^5	Takeuchi and Kohshima, 2004
AP-L	Livingston Island (Antarctic Peninsula)	62.39S 60.23W	13	*S. nivaloides*	4.9×10^8	This study

We used *in situ* algal cell concentration per area (cells m^{-2}) for model validation in this study. The algal data reported in previous studies had all been quantified using microscopic cell counts in the surface snow layer (top 2 cm). These data covered locations in NW Greenland (GL-Q; Onuma et al., 2018), Alaska (AK-K and AK-E, Takeuchi et al., 2006b; Takeuchi, 2013), Altai

(Russia; AT-A, Takeuchi et al., 2006a), Siberia (SB-S, Tanaka et al., 2016), Tienshan (China; TN-U, Tanaka, 2016), and Patagonia (PG-T, Takeuchi and Kohshima, 2004). Surface snow algal abundance data reported from Svalbard (Arctic Ocean; SV-W and SV-S, Stibal et al., 2007; Lutz et al., 2014), SE Greenland (GL-A, Lutz et al., 2014), Europe (EU-T, Remias et al., 2016), North America (NA-S, Painter et al., 2001), and New Zealand (NZ-A, Novis et al., 2002) were also used. Because most algal cell abundance data had been reported as algal cell concentration per unit of melt water volume (cells L^{-1}), we converted these data to algal cell concentrations per unit of area, assuming that the snow density was 500 kg m^{-3} and that the collected samples had been 2 cm deep.

We also used unpublished algal data obtained from snowfields in Japan (Mt. Tateyema) and the Antarctic Peninsula (Livingston Island), in 2012 and 2015 respectively. Mt. Tateyama (N 36.3°, E 137.4°) is an alpine snowfield above the tree line (1850–3000 m ASL), located in W Japan, and red snow algal blooming can be observed there annually as the snow pack thaws (May–July) (Segawa et al., 2005). We selected a snowy plateau called Raichozawa, located at 2300 m, as the study site (JP-T) because the snowpack here remained until early August. Livingston Island is located in the South Shetland Islands near the Antarctic Peninsula. The Spanish research station, Juan Carlos I (S 62.4°, W 60.2°), and the Hurd Peninsula ice cap (S 62.8°, W 60.8°) are located on the Hurd Peninsula, Livingston Island. Glaciological field observations have been conducted here to study the physical properties of ice on glacier dynamics, including surface mass balance and ice velocity on the ice cap (Navarro et al., 2013; Sugiyama et al., 2019). Red snow algal blooms can be found on the coastal snowpack on Livingston Island from January–February (Hodson et al., 2017). Our study site (AP-L) was located on the Livingstone Island coastal snowfield.

Temporal changes in the abundance of red snow algae were quantified using surface snow samples collected through d 117–217, in 2012, at JP-T, and during 6 sampling days during the period extending through d 19–30, in 2015, at AP-L. Samples were collected on each observation date from 3 to 10 randomly selected surface locations (0–2 cm depths), using a stainless-steel scoop. The sampling areas occupied ~ 100 cm^2 and were recorded for each collection. Samples were melted on-site and preserved in 3 % formalin in 30 mL clean polyethylene bottles before being transported to Chiba University, Japan, for analysis. Algal abundances were obtained from the water samples by counting cells and was represented as the cell number per unit surface area of snowpack (cells m^{-2}). This methodology has been described in more detail in previous studies, which included those in which field observations were carried out at sites GL-Q, AK-E, SB-S, AK-K, AT-A, TN-U, and PG-T, as shown in Table 1.

2.3. MATSIRO land surface model

We used the Minimal Advanced Treatments of Surface Interaction and Runoff land surface model (MATSIRO; Takata et al., 2003; Nitta et al., 2014, 2017) to evaluate temporal changes in snow algal abundance on snowfields worldwide. This model was developed to simulate land-based physical processes in a general circulation model, and six versions—the MATSIRO6, involving up to three snow layers, six soil layers (14 m in total), and a single canopy layer—were used for the Model for Interdisciplinary Research on Climate (MIROC6; Tatebe et al., 2019).

MATSIRO6 can simulate temporal and spatial changes in the snow water equivalent, snow cover fraction, and snow temperature. The snow water equivalent was simulated based on

the water balance, and in MATSIRO6 it was derived from the snowfall rate, snow sublimation, snowmelt, and refreezing of rainfall and snowmelt. The snow cover fraction was simulated using a lognormal distribution function for the subgrid snow water equivalent distribution, whereas the temperature of each snow layer was simulated using a thermal conductivity equation. The detailed methodology for calculating these physical properties of snow may be found in Nitta et al. (2014). Temporal changes in these snow physical properties have been validated using observations from various snowfields and derived from data for other land surface and snow physical models reported by the model intercomparison project (ESM-SnowMIP; Krinner et al., 2018). In this study, we used snow surface temperatures calculated using MATSIRO6 as input data for snow algal simulations at the study sites.

2.4. Atmospheric forcing for land surface modeling

The atmospheric conditions used in MATSIRO6 simulations were derived from atmospheric reanalysis data (Table 2). Various datasets for atmospheric reanalysis—which were derived from global atmospheric reanalysis data near the land surface, and bias-corrected using global meteorological observations—have been established for land surface modeling. In this study, we used the atmospheric conditions derived from the reanalysis dataset for each study site, because time-series meteorological observations were not always available.

The WFDEI forcing data set (Weedon et al., 2014) was used as the atmospheric conditions for land surface modeling in this study. This atmospheric reanalysis dataset includes three-hourly information on surface air temperature, surface air pressure, downward radiation (shortwave and longwave), humidity, wind speed, and precipitation rate. While this reanalysis data set is appropriate for land surface modeling at global or regional scales, high levels of uncertainty are present when it is used for meteorological conditions at specific elevations due to its rough horizontal resolution (0.5° × 0.5° globally).

For this reason, we applied elevation corrections to simulate temporal changes in snow algal abundance at specific sites. The surface air temperature at each site was corrected using elevation information and the original air temperature and by applying a temperature lapse rate,which was assumed to be - 6.5×10^{-3} Km^{-1}. The surface air pressure of each snowfield was corrected using elevation information and surface air temperature (before and after the correction), as recommended by the World Meteorological Organization (WMO-No. 8, in CIMO Guide, Part I, Chapter 3). The specific humidity at each site was corrected from the original data using the ratio of surface air pressure before and after correction, whereas the snowfall rate was corrected from total precipitation data, using the ratio of rain to snow, which itself was estimated using the surface air temperature, air pressure, and specific humidity given in MATSIRO6. The input and output data for the offline land simulation used to calibrate MATSIRO6 in this study can be seen in Table 2.

Table 2. Variables and parameters required for land surface modeling in this study

Variable or parameter	Description	Estimated Value	Unit
	Land surface model MATSIRO6		
Ta	Atmospheric temperature	Input	K
Qa	Atmospheric humidity	Input	kg kg^{-1}
Pa	Atmospheric pressure	Input	hPa
Ws	Wind speed	Input	m s^{-1}
Sw	Downward shortwave radiation	Input	W m^{-2}
Lw	Downward longwave radiation	Input	W m^{-2}
Pr	Total precipitation rate	Input	kg m^{-2} s^{-1}
Psn	Snowfall rate	Calculated	kg m^{-2} s^{-1}
Sn	Snow water equivalent	Calculated	kg m^{-2}
Tsn	Snow temperature	Calculated	K
Dsn	Snow density	Parameter	Kg m^{-3}
	Snow algae model		
X_0	Initial cell concentration	Parameter	cells m^{-2}
μ	Growth rate	Parameter	hour^{-1}
K	Carrying capacity	Parameter	cells m^{-2}
GP	Growth period	Calculated	hour
X	Algal cell concentration	Calculated	cells m^{-2}

2.5. Experimental design of snow algal growth simulation

To evaluate the algal model version as improved in this study, algal growth simulations (Ag-exp) were conducted under three different conditions at 15 sites, as shown in Fig. 1**c** and Table 1. The three conditions covered snow algal growth with: (1) the effect of snow melting only (X^M); (2) effects of snow melting and daylight length only (X^{MR}); and (3) effects of snow melting, day-light length, and snowfall (X^{MRF}) (Table 3). The atmospheric conditions for the land offline simulations were supplied by the WFDEI forcing dataset, which had been corrected for

study site elevations in advance.

Table 3. Overview of sensitivity tests applied in this study

Experiment ID	Initial cell Concentration X_0 (cells m^{-2})	Growth rate μ ($hour^{-1}$)	Carrying capacity K (cells m^{-2})	Atmospheric reanalysis data set
Algal growth simulation (Ag-exp)	6.33	0.018	Observation each site	WFDEI
Initial cell ensemble (X_0-exp)	$1.0 – 1.0 \times 10^3$	0.018	Observation each site	WFDEI
Growth rate ensemble (μ-exp)	6.33	0.01 – 0.025	Observation each site	WFDEI
Atmospheric reanalysis data set ensemble (Fd-exp)	6.33	0.018	Observation each site	WFDEI or GSWP3-FD or CRUJRA

The initial snow depth (in water equivalent) in MATSIRO6 was assumed at each study site to remain stable until the maximum algal cell concentration date. For example, the initial value was assumed to be 1000 kg m^{-2} for Arctic sites and 3000 kg m^{-2} for Japanese sites, which was consistent with snow depth observations (equal to 9 m in winter at JP-T, Osada et al., 2004). The snow surface temperature calculated using MATSIRO6 and the derived snowfall rate and solar radiation from atmospheric reanalysis data were used as input data for the snow algae model in this study.

Biological parameter data—such as initial cell concentration (X_0), growth rate (μ), and carrying capacity (K)—were not generally available for red snow algae in snowfields worldwide. To overcome this, we applied field observation values from the snowfield of a Greenlandic glacier, as reported by Onuma et al. (2018), for Ag-exp—and so X_0 and μ were assumed to be 6.33 cells m^{-2} and 0.018 h^{-1}, respectively. Maximum algal cell concentrations observed from the sites (Table 1) were used for K because the carrying capacity of red snow algae might vary for each snowfield, as suggested by Onuma et al. (2018).

Simulations were conducted from January 1 to December 31 each year at the study sites, except for the southern hemisphere sites NZ-A and PG-T, where 1998 and 1999 data for July 1 to December 31 were used.

We conducted more sensitivity testing on the updated snow algae model using two biological parameters—initial cell concentration (X_0-exp), and growth rate (μ-exp)—at each observation site (Table 3). Onuma et al. (2018) reported that the *S. nivaloides* initial cell concentration and growth rate were 6.33 and 694 cells m^{-2} and 0.39 and 0.42 d^{-1} (0.016 and 0.018 h^{-1}), respectively, at 2 sites on a Greenlandic glacier. Field observations suggested that *S. nivaloides* algal spores (cysts) were wind induced onto the snow surface during the early melting season, and they assumed that the initial cell concentration consisted of these wind-supplied algal spores before on-site algal growth initiation. Based on a previous study, the range for the initial cell concentrations (X_0-exp) was assumed for sensitivity testing to be between 1–1000 cell m^{-2}. Because snow algae growth rates vary between snowfields worldwide, it had been suggested previously that the sensitivity of the snow algae model to growth rates should be investigated. Previous studies have reported that *C. nivalis* growth rates, as obtained from field observations and cultivation, were 0.22 (Onuma et al., 2016) and 0.60 d^{-1} (Leya et al., 2009). Based on these data, we assumed that the *μ-exp* growth rate ranged between 0.01–0.025 h^{-1}. The maximum algal cell concentration observed from the study sites was assumed to be *K*, for both X_0-exp and μ-exp, the same as for Ag-exp.

In addition to applying sensitivity testing to biological variables, we reviewed model sensitivity to four atmospheric conditions. Although temporal changes in snow algal abundance may be affected by snow physical or atmospheric conditions, the quantitative effect of such conditions on algal cell abundance remained uncertain. Therefore, Fd-exp, which is an ensemble simulation using the WFDEI, GSWP3-FD, and CRUJRA forcing datasets, was conducted in this study, to review the sensitivity of algal growth to atmospheric conditions (Table 3). GSWP3-FD (Hurk et al., 2016; Kim, 2017) and CRUJRA (Harris, 2019) forcing datasets provided the different atmospheric conditions, and an overview of the three datasets, including WFDEI, can be seen in Table S1. The surface air temperature, surface air pressure, and specific humidity data from GSWP3-FD and CRUJRA were corrected using each site's elevation, as was WFDEI. The initial cell concentration, growth rate, and carrying capacity were taken as 6.3 cells m^{-2}, 0.018 h^{-1} and the observed maximum cell concentration (cells m^{-2}) for Fd-exp, respectively. The experimental architecture for the sensitivity tests used in this study has been summarized in Table 3.

To evaluate snow algae model sensitivity to biological variables and atmospheric conditions, we used the two variables visible cell concentration of algal bloom (VCAB), and the reaching time to the algal bloom (RTAB). In this study, VCAB was defined as 5.0×10^5 cells m^{-2} because this was the minimum algal cell concentration for a red snow phenomenon observed on a Greenland glacier by Onuma et al. (2018) and was comparable to algal bloom concentrations observed in other areas (e.g., 2.2×10^6 cells m^{-2} at AT-A, 1.3×10^6 cells m^{-2} at TN-U, and 6.0×10^5 cells m^{-2} at PT-G). The time taken to reach the VCAB was defined as the RTAB, and if a calculated algal cell concentration did not reach the VCAB in a simulation, the date of the calculated maximum abundance was still defined as the RTAB.

3 Results

3.1. Simulation and evaluation of algal cell concentrations achieved using the original snow algae model

The algal growth simulations, Ag-exp, produced RTABs ranging from d 155–220; the date depended on their Northern Hemisphere locations, with mid-latitude site RTABs being generally earlier than those for polar sites. Specifically, the RTAB ranged from d 155– to 220 (early June to early August), at the Northern Hemisphere mid-latitude sites (N 30–60°; AT-A, EU-T, TN-U, NA-S, and JP-T), and from d 175–220 for the polar sites (N 60–90°; SV-S, SV-W, GL-Q, GL-A, AK-E, AK-K, and SB-S). The algal cell concentration, X^M, at JP-T, which was calculated using snow melting duration only, showed no significant increase from d 1–70, and then increased, reaching VCAB on d 155 (RTAB = d 155) (Fig. 3). X^M values for mid-latitude sites were found to reach the VCAB earlier than the polar sites. Similarly, X^M at Southern Hemisphere mid-latitude sites (S 30–60°; NZ-A and PG-T) reached the VCAB earlier than it did at the single Southern Hemisphere polar site (S 60–90°; AP-L). The RTAB estimated from X^{MR}, which was calculated from the duration of snow melting under daylight conditions, did not significantly differ from that estimated at the study sites using X^M (Fig. 3).

346

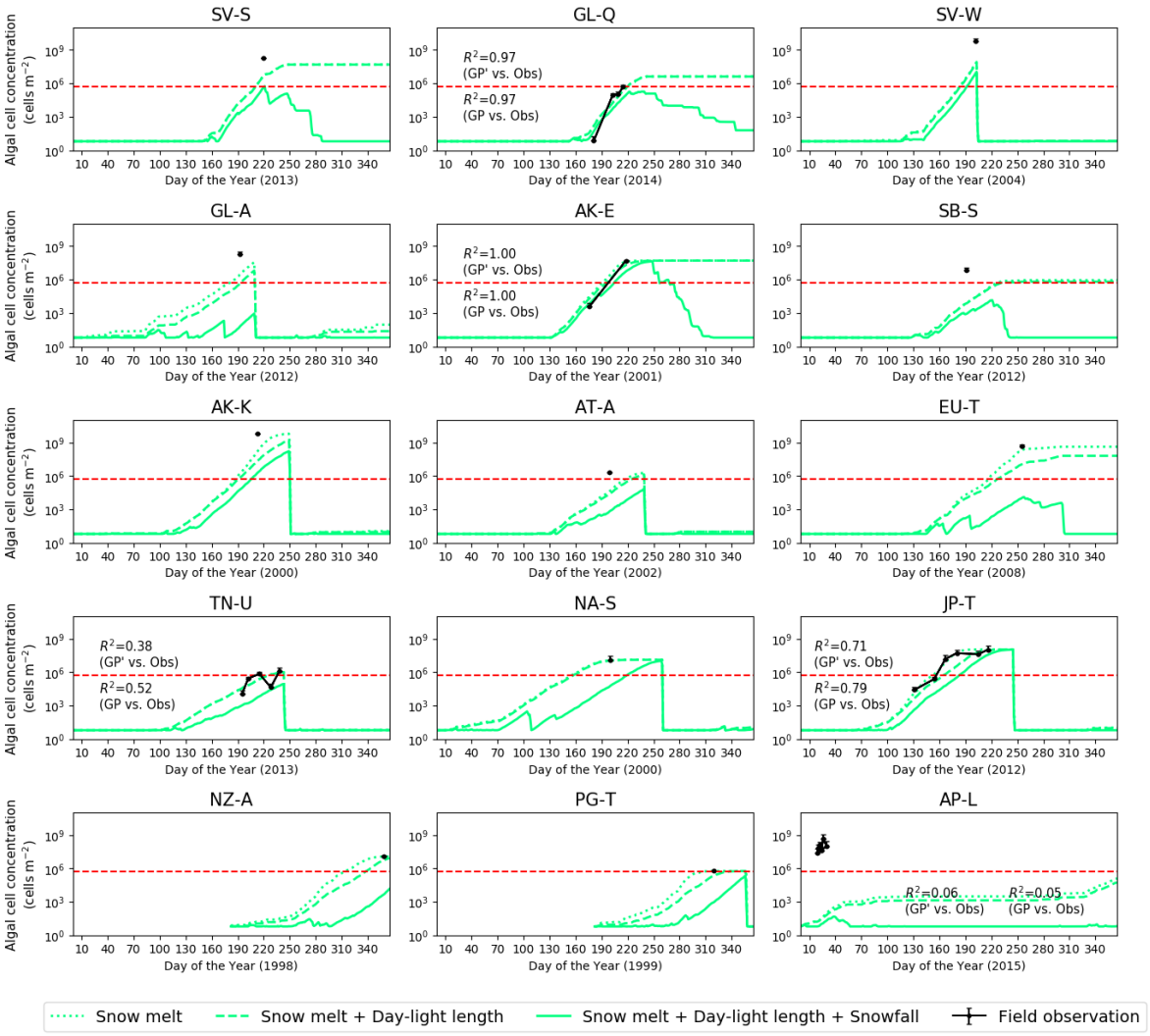

347

348 **Figure 3**. Temporal changes in red snow algal cell concentrations at each site. Dotted, dashed
349 and solid lines indicate X^{M}, X^{MR} and X^{MRF}, respectively

350

351 The simulation achieved using the original snow algae model showed algal cell
352 concentration changes over time which agreed with *in situ* values for snowfields at GL-Q, AK-E,
353 TN-U, and JP-T. For example, Ag-exp showed that the RTAB estimated for GL-Q from X^{M} was
354 d 215, which was the same date that the maximum cell concentration was observed at the site
355 (Fig. 3). The RTABs for sites AK-E, EU-T, TN-U, JP-T, and NZ-A also agreed well with the
356 observations, whereas the changes in X^{MR} over time did not significantly differ from those for
357 X^{M}, at any of the sites. The determination coefficients for temporal change in X^{M} (and X^{MR}),
358 compared with those for the observed algal cell concentrations, were 0.97 ($P < 0.05$), 1.00 ($P <$
359 0.05), 0.38 ($P > 0.05$), and 0.71 ($P < 0.05$), at GL-Q, AK-E, TN-U, and JP-T, respectively.

3.2. Simulation and evaluation of algal cell concentrations achieved using the improved snow algae model

RTABs simulated using the updated snow algae model ranged from d 180–240 in the Northern Hemisphere, showing that the snow algal bloom timing estimates were significantly later than those simulated using the original snow algae model, at all sites. For example, the algal cell concentration, X^{MRF}, at JP-T, which was simulated using snow melting, daylight length, and interruption by new snow cover effects, kept X_0 from d 1–100, and then reached the VCAB on d 180 (RTAB = d 180) (Fig. 3). The RTAB ranged from d 180–255 (late June to early September) at the Northern Hemisphere mid-latitude sites, and from d 185–220 in the polar sites. In Southern Hemisphere, RTABs were 365, 355, and 40, at sites NZ-A, PG-T, and AP-L, respectively. These results showed that RTABs for X^{MRF} were later than had been the case for X^{M} and X^{MR}. We also saw that there were no significant differences in the RTABs estimated using X^{MRF} among the sites at different latitudes, unlike the case for those estimated using either X^{M} or X^{MR}.

Snow algal abundances simulated using the updated model produced seasonal change results which agreed better with observational data than those simulated using the original snow algae model. Ag-exp showed that X^{MRF} at GL-Q started to increase on d 175 and then reached the VCAB on d 220. The temporal changes estimated using X^{MRF} agreed with the site observation data better than those achieved using either X^{M} or X^{MR} (Fig. 3). The determination coefficients for the temporal change in X^{MRF} against the observation data were 0.97 ($P < 0.05$), 1.00 ($P < 0.05$), 0.52 ($P > 0.05$), and 0.79 ($P < 0.05$), for sites GL-A, AK-E, TN-U and JP-T, respectively. These coefficients were slightly higher than those for the X^{M} and X^{MR}, whereas the RTABs calculated using X^{MRF} agreed with the timing of the red snow phenomenon observed at the other sites, including SV-S, SV-W, EU-T, NA-S, NZ-A, PG-T, and AP-L.

3.3. Model sensitivity testing in relation to biological parameters and atmospheric conditions

Testing X_0-exp sensitivity to the initial algal cell concentration showed that the RTAB was approximate 15–30 d earlier where the initial cell concentration was 100-fold greater than the original concentration (1.0 cells m^{-2}, Fig. 4**a**). For example, the RTABs in the simulation of the minimum initial cell concentration (1.0 cells m^{-2}) were on d 215 and 195, at AK-E and JP-T, respectively. Simulation results showed that the AK-E RTABs were on d 200, 180, and 175, for the cases in which the minimum initial cell concentrations increased by a factor of 10, 100, and 1000, respectively. Under similar circumstances, the RTABs for JP-T were on d 180, 160, and 145. X^{MRF} did not reach the VCAB before the disappearance of snow in either GL-A or AP-L, in any of the simulations.

The test of μ-exp sensitivity to algal growth rate showed that, in the case of a 10 % greater growth rate, the RTAB was approximately 10 d earlier than the original rate (Fig. 4**b**). RTABs simulated using a growth rate of 0.018 h^{-1} (original case) were 210 and 180 d at AK-E and JP-T, respectively. The RTABs at AK-E were simulated to be d 200, 195, and 190, for growth rates 10, 20, and 30 % greater than that of the original rate, respectively. Under similar circumstances, the JP-T RTABs were simulated to be d 170, 160, and 155. X^{MRF} did not reach the level of algal blooming at GL-A, SB-S, EU-T, NZ-A, or AP-L, in any of the simulations.

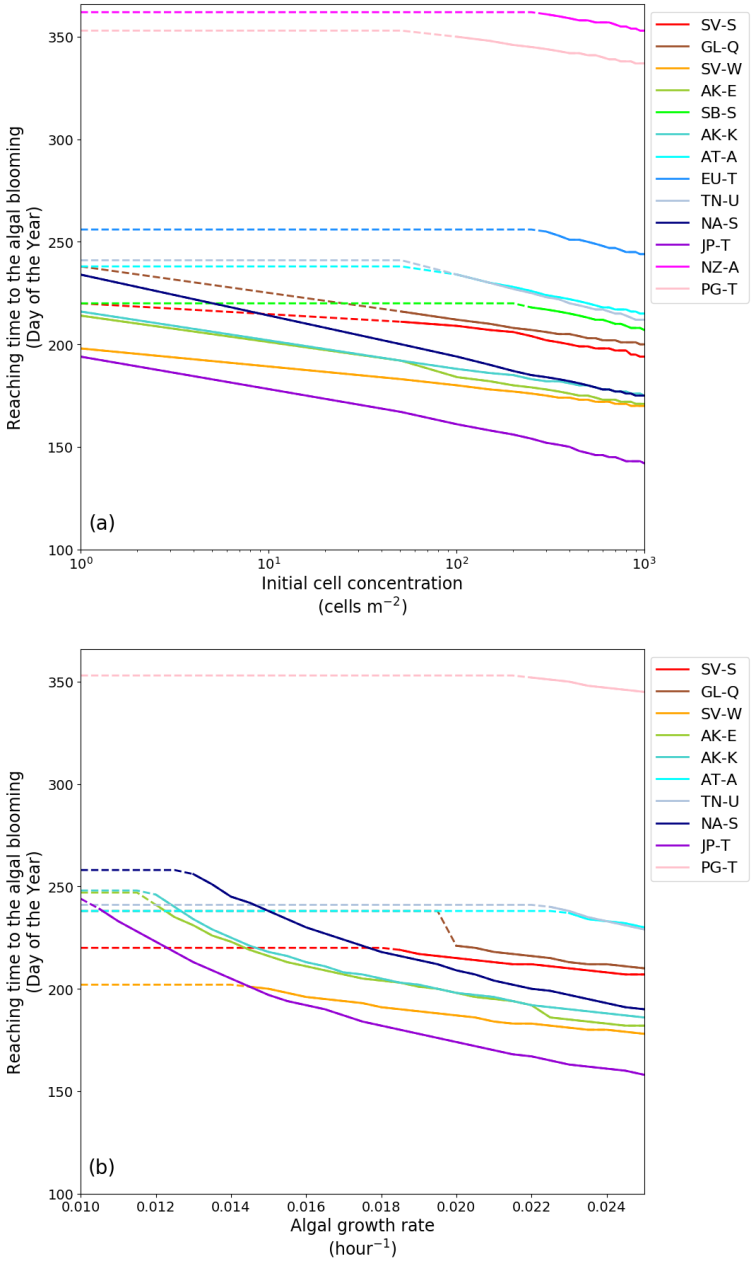

Figure 4. Sensitivity of snow algal growth rate to biological parameters at each site: **a** initial cell concentration sensitivity; **b** algal growth rate sensitivity

Testing Fd-exp sensitivity to atmospheric conditions showed that the RTAB estimate results significantly varied among the atmospheric reanalysis datasets, even at the same site. The minimum, median, and maximum RTABs, derived from simulations using the WFDEI, GSWP3-FD, and CRUJRA datasets, can be seen for each site in Fig. 5—which also shows the atmospheric reanalysis data set uncertainties for the RTABs. The RTABs varied significantly among the data sets at sites SV-S, GL-A, SB-S, AT-A, EU-T, TN-U, and NA-S. The differences in the RTABs estimated between the data sets were equal to 100 d at EU-T and just 5 d at site JP-T.

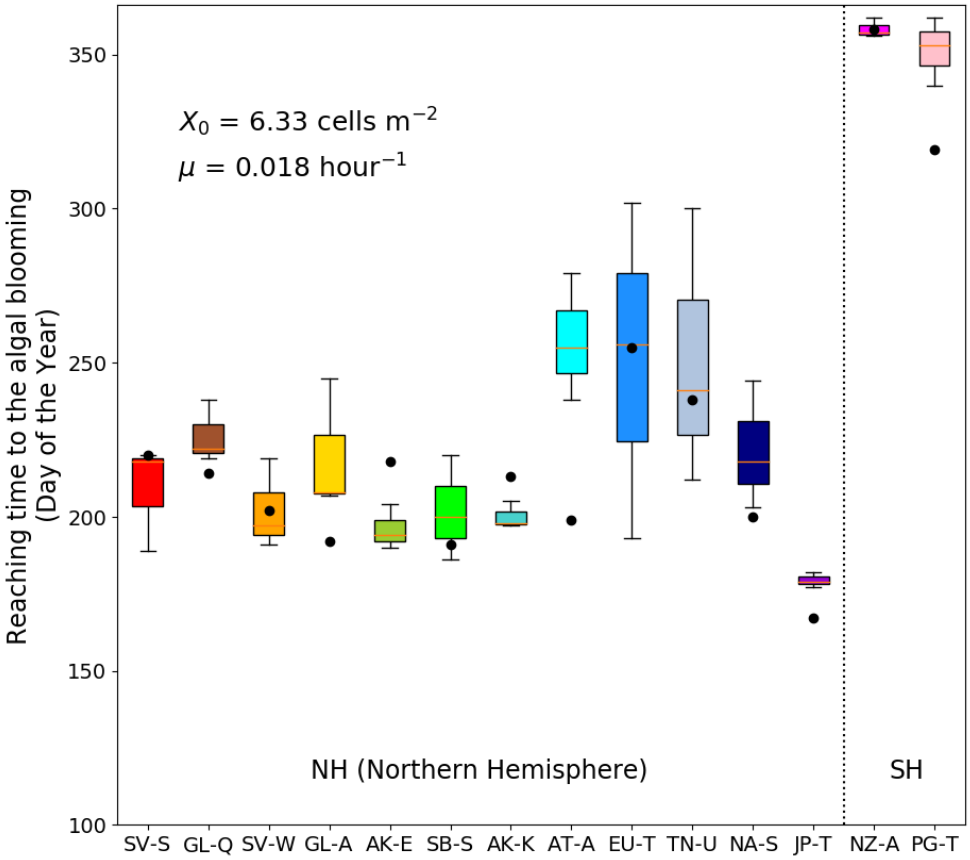

Figure 5. Modeled algal growth uncertainties under different meteorological conditions

4 Discussion

4.1. Effect of daylight length on algal bloom simulation results

The simulations showed that RTABs did not differ significantly in cases where daylight length was or was not taken into account, indicating that daylight length did not affect snow algal bloom timing to a significant extent. Ag-exp showed that GP^{M}, which represents cumulative snow melting time, was longer than GP^{MR}, excluding night time (Fig. S1). In the simulations, surface snow could melt at night when the daily surface air temperature was > 10 ℃ at mid-latitude sites (Fig. S2). However, even if the surface snow had melted, snow algae would be unlikely to grow during the night because they cannot not photosynthesize without solar radiation. In experimental studies, the snow algae *Cr. tughillensis* and *Cr. chenangoensis* showed the greatest increases in response to the longest daylight scenario (light:dark 24:0 h) (Hoham et al., 2000, 2009), suggesting that snow algal growth depended on daylight length. Hence, GP^{MR}, excluding nighttime, was expected to simulate algal growth better than GP^{M}—however, there were no significant differences in the RTABs calculated using X^{M} and X^{MR}, at any site (Fig. 3). This indicated that snow did not melt during the night before algal blooming commenced. The atmospheric reanalysis data set showed that surface air temperatures often fell below freezing during the night in the early melting season, indicating that snow melting during the night would have been rare.

435 4.2. Effect of snowfalls on algal bloom simulations

436 Updated model simulations which included the effects of snowfall and daylight length
437 were more accurate than those produced using the original model, at most sites, suggesting that
438 snowfall significantly affected algal growth, including algal bloom timing. The RTAB in the
439 case of X^{MRF} was later than it was the case of X^{MR}, at all sites (Fig. 3), whereas comparing
440 temporal changes in the X^{MRF} with those in the X^{MR} showed that the rate of increase in X^{MRF}
441 declined due to frequent snowfall during the early melting season at the study sites. For example,
442 daily surface air temperature at site JP-T first exceeded 0 ℃ on d 90, but snowfalls continued to
443 occur quite frequently, up to d 110. The algae gradually increased from d 90 to 110 at this site, in
444 the case of X^{MR}, whereas X^{MRF} showed no increase during the same period. These results
445 indicated that frequent snowfall events delayed the RTAB. Model simulations showed that
446 increasing trends in X^{MRF} agreed well with observed algal cell concentrations at sites GL-Q, AK-
447 E, TN-U, and JP-T (Fig. 3). Figure 6 indicates that the updated snow algae model was generally
448 more accurate than the former model at many study sites, suggesting that incorporating snow
449 cover on the algal growth surface had improved model accuracy. Although the effect of snowfall
450 on an algal surface had been previously reported (Tanaka, 2016; Onuma et al., 2016), it had not
451 been quantified in field observations. Further periodical observations during the early snow
452 melting season are now needed to further improve spring to summer snow algal bloom prediction
453 accuracy.
454

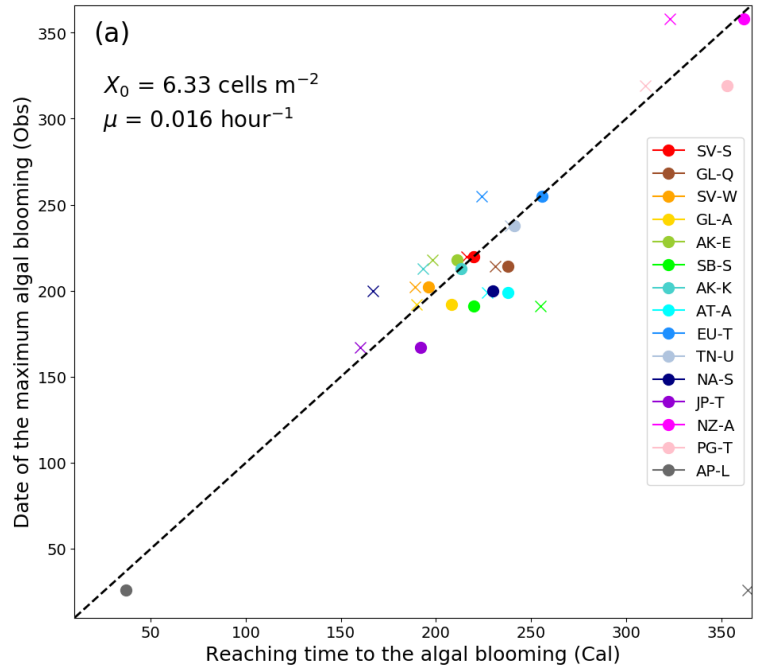

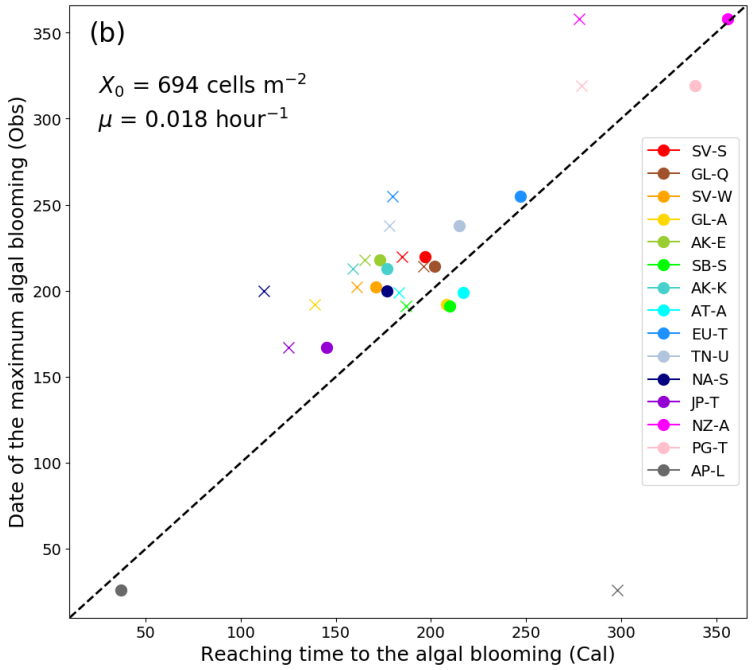

Figure 6. Comparison between simulated and observed algal bloom timing. Solid marks and crosses represent results from the updated and original snow algae bloom models, respectively

4.3. Sensitivity of algal growth simulation to initial cell concentration and growth rate

Testing biological parameter sensitivity suggested that the initial snow algae cell concentrations and growth rate estimates in each test were significantly affected by the RTAB. In this study, we conducted simulations using the updated snow algae model with an initial cell

concentration of 6.33 cells m^{-2}, and a growth rate of 0.018 h^{-1}. However, these parameters may have introduced some uncertainty, as they were derived using *in situ* Greenland glacier data (Onuma et al., 2018). *S. nivaloides* blooming was previously reported as appearing on d 180 and 215 at two different sites, with the initial cell concentration and the growth rate at the former site (694 cells m^{-2} and 0.018 h^{-1}) higher than those at the latter site (6.33 cells m^{-2} and 0.016 h^{-1}). Differences in biological parameters would cause uncertainty in the timing of snow algal blooming, and thus, we quantified the range of RTAB uncertainty which could be attributed to the biological parameters observed in the previous study.

RTABs simulated using the highest (694 cells m^{-2} and 0.018 h^{-1}) and lowest (6.33 cells m^{-2} and 0.016 h^{-1}) reported biological parameters can be seen in Figs 6**a** and 6**b**, respectively, where it can be seen that the RTABs in Fig. 6**b** were 10–30 d earlier than those in Fig. 6**a**. Snow algal blooming was generally observed on the day between the RTABs in Figs 6**a** and **b**, suggesting that the RTAB simulated with the updated snow algae model changed by approximately 10 d, compared with the observed blooming date of the snow algae. Although snow algae initial cell concentrations and growth rates may depend on the amount of mineral dust supplied from the atmosphere and on nutrient conditions (nitrogen and phosphorus), as suggested by Onuma et al. (2016; 2018), the major factors affecting the biological parameters remain uncertain. Field data on snow algae biological parameters from various snowfields and glaciers worldwide are needed. However, our simulations suggested that the updated snow algae model could forecast snow algal bloom timing with an accuracy of approximately 10 d.

Sensitivity testing suggested that the RTAB range was likely to be related to site latitude. For example, the RTAB at JP-T (36° N) ranged from d 145–195, whereas at SV-W (77° N), it ranged from d 180–200 in X_0-exp (Fig. 4**a**). Similarly, the RTAB at JP-T ranged from d 160–250, whereas it ranged from d 180–200 in µ-exp (Fig 4**b**). These differences in the RTAB among the sites could be explained by their different GP^{MRF} results. GP^{MRF} accumulated during the daytime only at JP-T, whereas at site SV-W, it also accumulated during the night (Fig S1). The sensitivity tests showed similar trends at the other sites. At polar sites, snow algae are likely to grow for a shorter period because of the longer daylight length during summer, leading to a shorter range for the RTAB in each sensitivity test. For example, the RTAB simulated with the initial cell concentration of 694 cells m^{-2} was 15 d earlier than that simulated using 6.3 cells m^{-2} at SV-W and 30 d earlier in the case of JP-T. In µ-exp, the RTAB with a growth rate of 0.018 h^{-1} was 10 d earlier than that simulated with an initial cell concentration of 0.016 h^{-1}, at SV-W, whereas it was 25 d earlier in the case of JP-T. Although differences in biological parameters could lead to uncertainty in algal bloom timing, the uncertainty may be smaller in polar regions than in mid-latitude regions. The results here suggested that the timing estimates for the red snow phenomenon achieved using the updated snow algae model were more reliable at polar sites.

4.4. Algal bloom simulation uncertainties caused by different atmospheric reanalysis data sets

Fd-exp showed that sensitivity to meteorological conditions was higher in the Asian high mountain areas than in polar snowfields, suggesting that RTAB estimation uncertainty was larger in areas where precipitation mainly occurred in summer. RTABs simulated with the updated snow algae model using the WFDEI, GSWP3-FD, and CRUJRA atmospheric reanalysis datasets varied greatly at some sites (Fig. 5). Notably, the difference in the RTAB between the 25^{th} and 75^{th} percentiles was 50 d at sites EU-T and TN-U. The differences were smaller, approximately

20 d, at some alpine sites (SB-S, AT-A, and NA-S) and polar maritime snowfield sites (SV-S, SV-W, and GL-A). This RTAB difference was probably due to the frequency of snowfall during summer in each dataset. As reported previously, most Asian high mountain glaciers are characterized by summer accumulation due to the influence of the Asian monsoon (Fujita and Ageta, 2000; Fujita, 2008; Sakai and Fujita, 2017). According to meteorological conditions derived from the atmospheric reanalysis data sets, study sites SB-S, AT-A, EU-T, and TN-U could probably be classified as summer accumulation-type glaciers (Figs S2 and S4). The higher sensitivity of the RTAB to atmospheric conditions was probably caused by frequent summer snowfalls at these sites, which would greatly affect the algal growth in the X^{MRF}. Furthermore, a previous study showed that precipitation amounts derived from atmospheric reanalysis datasets still have levels of uncertainty in high elevation and polar maritime areas (Weedon et al., 2014). Large RTAB variations may also be influenced by dataset accuracy at specific sites—although there were no significant differences in the RTABs estimated using the different datasets at sites GL-Q, AK-E, and JP-T. The determinant coefficient in the algal cell concentrations achieved by simulation and observation at these sites was > 0.8 (Fig. 4), suggesting that the updated snow algae model was capable of reproducing red snow bloom timing in these regions, even if the dataset contained uncertainties regarding atmospheric conditions. Notably, the updated snow algae model performed very reasonably in reproducing snow algal bloom timing at sites where the atmospheric reanalysis data were highly accurate.

The model needs to be improved if it is to reproduce red snow blooming accurately on a global basis—especially in summer accumulation-type glaciers. At such sites, model validation using *in situ* observational meteorological conditions would be necessary. It has also become apparent that the level of snow algal bloom sensitivity to meteorological conditions in summer may vary depending on seasonal precipitation patterns. Further, the snow algae model could be a useful tool for revealing snow algal growth sensitivity to meteorological conditions.

4.5. Other possible factors affecting red snow algal blooming

The current status of snow algal growth numerical modeling in snowfields has been summarized in this section, with aspects of the updated snow algae model which still require improvement being identified. The updated model can estimate algal bloom timing better than what had been achievable in simulations using the previous model (Onuma et al., 2018) at comparable sites (Fig. 6). As noted in 4.2, this was probably due to incorporating the effect of snowfall on algal abundance in surface snow into the model. The result also showed, however, that algal cell concentrations simulated using the updated model underestimated observed concentrations at the study sites, resulting in algal blooming not appearing during the thaw season at the polar sites GL-A, SB-S, and AP-L. This may be attributed to uncertainties in both the biological parameters and the atmospheric reanalysis data (especially those for snowfall amount and frequency) at the sites. Other biological process issues may also be contributing to these underestimations. Previous studies have suggested that snow algae motile cells could swim up to the snow surface from the soil, or from ice below the surface snow (Müller et al., 2001; Remias, 2012). The snow depth at site AP-L ranged from 5–20 cm during the observation period, and thus, as Müller et al. (2001) suggested that such motile cell vertical movement occurred at snow depths < 40 cm, snow algal cells originating from the ground may have contributed to underestimating the simulated algal cell concentration at AP-L. We need to consider incorporating such biological processes into snow algae models in the future. Although the snow algae model could simulate temporal changes in cyst cell concentrations, some of these cells

might transform into vegetative cells during the thaw (Remias, 2012). Further field observation and cultivation are needed to quantify such algal stage changes so that they can be incorporated into the snow algae model.

Overall, we have concluded that challenges remain in the effective and accurate reproduction of snow algal abundance temporal changes using the updated snow algae model presented here. Despite this, we have, however, been able to demonstrate that the snow algae model reasonably reproduced algal bloom start times at the study sites, from which we can conclude that the snow algae model has the potential to predict the appearance of red surface snow worldwide.

4.6. Global simulation of red snow algae blooms

Based on evaluating algal cell abundance and bloom timing using the updated snow algae model in the previous sections, we incorporated the snow algae model described in Section 2.1 into a scheme of snow physical processes in MATSIRO6. We named this version for snow algal simulation Bio-MATSIRO, using the same naming convention applied to the water isotope simulation, Iso-MATSIRO, by Yoshimura et al. (2006). Bio-MATSIRO can be used to calculate temporal changes in algal cell concentration (cells m^{-2}) at regional and global scales, using atmospheric conditions near the land surface as input data. The model input data for simulations using Bio-MATSIRO in this work have been summarized in Table 2.

To evaluate snow algal seasonal growth changes and global distribution qualitatively, we conducted a two-dimensional offline land simulation, using Bio-MATSIRO. For this, we conducted three global simulations, using Bio-MATSIRO with the WFDEI, GSWP3-FD, and CRUJRA data sets. The horizontal resolution and calculation period for these simulations were 0.5° and from January 1, 1980 to December 31, 2014, respectively, to ensure that we had common horizontal resolutions and data periods for the three data sets. Land physical properties, such as snow water equivalent, were derived in advance from spin-up simulations (35 y total), using the same reanalysis data set, and were used as initial conditions for the three simulations. The initial cell concentration and algal growth rate were the same as Ag-exp in this study (6.33 cells m^{-2}, and 0.018 h^{-1}, respectively) because these preliminary biometrics seemed to facilitate better model simulation performance. As there is little information available on carrying capacity, which is likely to vary between sites (snowfields or glaciers) and years, it was assumed to be 3.5×10^7 cells m^{-2}, which was the carrying capacity suggested by Onuma et al. (2018), for Greenlandic Glacier sites.

The global simulation established using Bio-MATSIRO showed that snow algae grew from spring to summer in both hemispheres, and that their blooming sites were generally consistent with red snow sites reported previously, suggesting that Bio-MATSIRO had the potential to reconstruct snow algal blooms at the global scale. The global distribution of snow algal blooming was derived from the monthly means of the X^{MRF} (1980–2014 climatological mean), which were the algal cell concentrations simulated with Bio-MATSIRO using each atmospheric reanalysis data set. Red snow blooming (X^{MRF}, atmospheric reanalysis data set: WFDEI) distribution for each month's snow cover can be seen in Fig. 7. In the Northern Hemisphere, snow algae gradually increased from March to August, and their blooming area gradually extended from mid- to high-latitude areas. The area covered by the red blooms then extended southward because snowfall events frequently occurred in high latitudes. Red snow algal blooming simulated with Bio-MATSIRO appeared between June and August, and the

blooming area agreed well with the red circles (red snow phenomenon reported by previous studies) shown in Fig. 1. Red snow in European and North American snowfields had been reported previously over periods extending from summer to early autumn (Thomas and Duval, 1995; Remias et al., 2016), and the reported areas were consistent with simulated red snow algal bloom areas. In the Southern Hemisphere, the model simulation presented red snow algae gradually increasing from September to March, especially in Patagonia and on the Antarctic Peninsula. The red snow phenomenon has been reported as occurring between November and March in these regions (Takeuchi and Kohshima, 2004; Gray et al., 2020). Interestingly, the red snow algal bloom simulation hardly showed any occurrences in either N Russia or NW Canada—and there have actually been few reports of this phenomenon there. Frequent snowfall events during the snow melting season would interrupt snow algal bloom appearance in these regions because X^{MRF} drastically decreased to X_0 in August. Simulations using GSWP3-FD and CRUJRA showed spatial and seasonal changes in X^{MRF} similar to those simulated using WFDEI (Figs S5 and S6), with these results suggesting that Bio-MATSIRO had the potential to reproduce seasonal and geographical changes in red snow algal abundance globally.

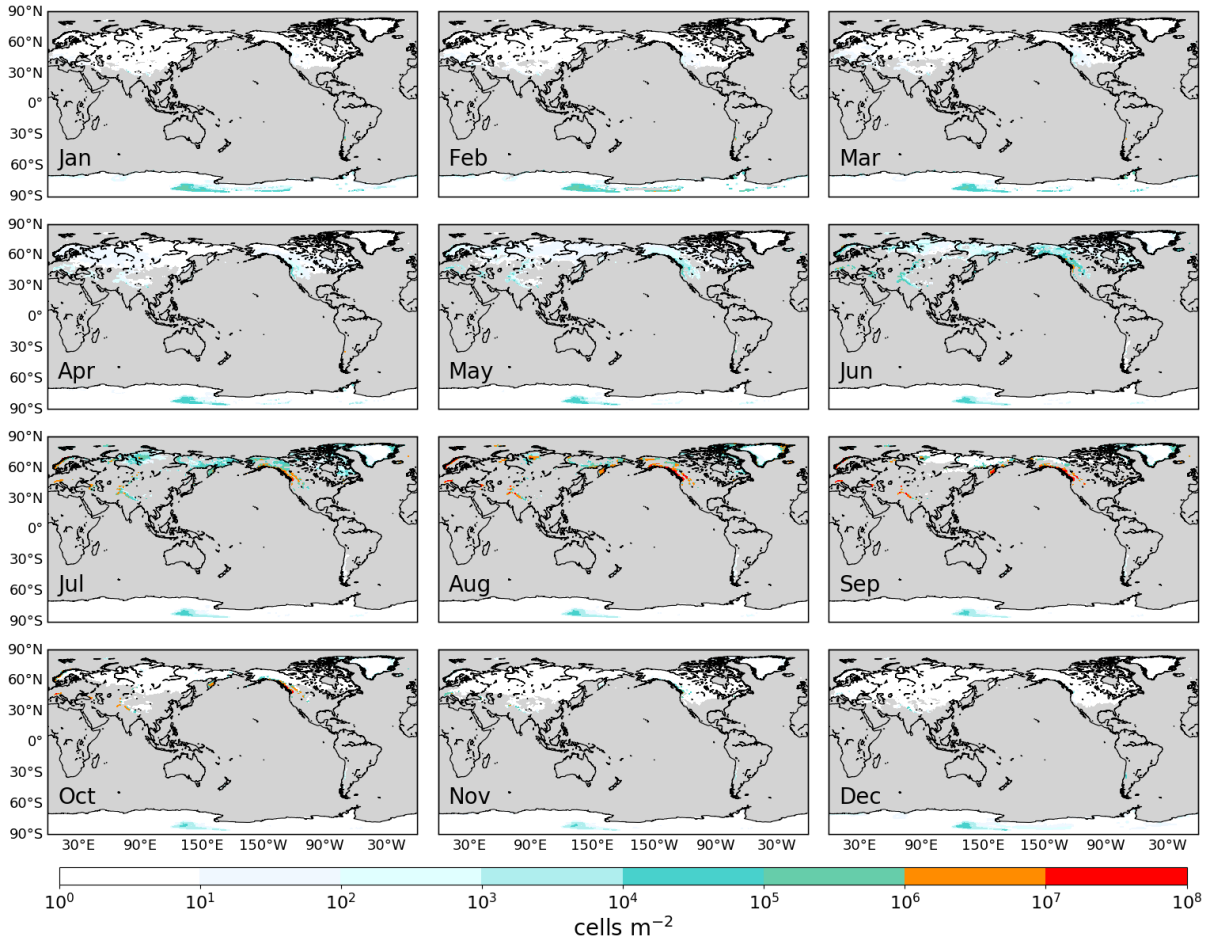

Figure 7. Distribution of red snow algal abundance on the surface snow, as simulated using the land surface model with the atmospheric reanalysis data set WFDEI (1980–2014)

Because we used constants for the biological parameters (initial cell concentration, growth rate, and carrying capacity) and atmospheric reanalysis data at the scale of 0.5° globally, the algal cell concentrations derived from our simulations contained some uncertainty levels in this study. Further observational and modeling studies are necessary to improve the snow algae model. Satellite observations of red and green snow algae blooms have been conducted recently (Hisakawa et al., 2015; Ganey et al., 2017; Huovinen et al., 2018; Gray et al., 2020; Khan et al., 2021), and validating model simulations with satellite observations would also be useful, at the glacial or regional scales. In addition, global simulation of red snow algal blooming, using a land surface model, could provide an important contribution to understanding climate change effects on snow and ice distribution in time and space.

5 Conclusions

We updated the existing snow algae model based on observational data from 15 snowfields and incorporated it into a land surface model to quantify time and space changes in snow algal abundance worldwide. The existing snow algae model (Onuma et al., 2018) could simulate temporal changes in the abundance of red snow algae in surface snow, using snow temperature, but up until now had only been applied to simulate the abundance of Greenlandic glacier snowpack. In this study, the effects of daylight length and snowfall rate on algal cell abundance were incorporated into the model, and the revised model simulations achieved good agreement with observations at snowfields worldwide, from polar to mid-latitude areas—particularly in regions with fewer summer snowfalls.

Based on these encouraging results, we incorporated the updated snow algae model into a land surface model and conducted a global snow algal simulation, using Bio-MATSIRO. This simulation produced results showing prominent algal blooms taking place in areas generally consistent with regions where the red snow phenomenon had been reported in either *in situ* or satellite observations. Our simulations suggested that Bio-MATSIRO has the potential to simulate temporal and spatial changes in red snow algal abundance and to predict the timing and coverage of the red snow phenomenon.

Snow algal distribution may be a key to revealing the geographic specifications of microbes worldwide (Lutz et al., 2016; Segawa et al., 2018; Procházková et al., 2019; Zawierucha and Shain, 2019). The snow algae model may be useful not only for providing such biological information but also for quantifying snow algal contributions to thaw events worldwide (by reducing snow surface albedo), revealing trends over time. This contribution has been reported in many studies as a bioalbedo effect and has been quantified using *in situ* observations, satellite observations, and numerical simulations (Thomas and Duval, 1995; Painter et al., 2001; Takeuchi et al., 2006b; Aoki et al., 2013; Lutz et al., 2016; Cook et al., 2017; Ganey et al., 2017; Mauro et al., 2017; Gray et al., 2020; Onuma et al., 2020). Because these studies focused on specific mountains or glaciers, comprehensive bioalbedo effects should be investigated at the global scale in the future using numerical simulation. To simulate bioalbedo effects at such a scale, a numerical bioalbedo model that has the capacity to calculate snow albedo (with the effect of snow algae included) needs to be incorporated into land surface models and climate models. Although further observations and simulations would further improve snow algae models, our study has provided an important first step towards revealing the global geographic characteristics of snow algae and their contribution to snow melting.

Author contributions

YO, KY, and NT designed the study and the paper. YO and NT collected snow samples and quantified snow algal abundance. YO developed the snow algae model and prepared the atmospheric reanalysis data at the validation sites, then conducted the numerical model simulation.

Acknowledgments

This work was supported by the Integrated Research Program for Advancing Climate Models (TOUGOU) Grant Number JPMXD0717935457 from the Ministry of Education, Culture, Sports, Science and Technology (MEXT), Japan. This study was also supported in part by Grant-in-Aids (JP23221004, JP26247078, JP26241020, JP16H01772, JP16H06291, JP19H01143, JP20K19955), the Arctic Challenge for Sustainability (ArCS, JPMXD130000000) and the Arctic Challenge for Sustainability II (ArCS II, JPMXD1420318865). We thank the Spanish Polar Program for the support provided by the Juan Carlos I Station on Livingston Island. Project CTM2014-56473-R from the Spanish Polar Program contributed to the funding of the field work on Livingston Island. Thanks to Dr. Francisco J. Navarro and Dr. Shin Sugiyama, who supported the field observation. We also thank Dr. Hajime Iida and Dr. Kotaro Fukui, who supported a field observation in Mt. Tateyama.

Data Availability

All of the observation data, output data and scripts for the figures in this study are available at the following DOI.
doi.org/10.5281/zenodo.4626347

Supporting Information

Supporting tables and figures are uploaded separately.

References

Aoki, T., Kuchiki, K., Niwano, M., Kodama, Y., Hosaka, M., & Tanaka, T. (2011), Physically based snow albedo model for calculating broadband albedos and the solar heating profile in snowpack for general circulation models. *J. Geophys. Res.*, 116, D11114. doi:10.1029/2010JD015507

Aoki, T., Kuchiki, K., Niwano, M., Matoba, S., Uetake, J., Masuda K., & Ishimoto, H. (2013), Numerical Simulation of Spectral Albedos of Glacier Surfaces Covered with Glacial Microbes in Northwestern Greenland. RADIATION PROCESSES IN THE ATMOSPHERE AND OCEAN (IRS2012), Robert Cahalan and Jürgen Fischer (Eds), *ALP Conf. Proc.*, 1531, 176. doi:10.1063/1.4804735

Cepák, V., Kviderová, J., & Lukavský, J. (2016), The first description of snow algae on Mount Olympus (Greece). *Nova, Hedwigia*, 103:457–73. doi:10.1127/nova_hedwigia/2016/0365

CIMO Guide, Part I, Chapter 3, https://www.wmo.int/pages/prog/www/IMOP/CIMO-Guide.html

Cook. J. M., Hodson, A. J., Taggart, A. J., Mernild, S. H., & Tranter, M. (2017), A predictive model for the spectral "bioalbedo" of snow. *J. Geophys. Res. Earth Surf.*, 122. doi:10.1002/2016JF003932

Curl Jr., H., Hardy, J. T., & Ellermeier, R. (1972), Spectral absorption of solar radiation in alpine snow fields. *Ecology*, 53, 1189–1194. doi:10.2307/1935433

Decharme, B., Brun, E., Boone, A., Delire, C., Le Moigne, P., & Morin, S. (2016), Impacts of snow and organic soils parameterization on northern Eurasian soil temperature profiles simulated by the ISBA land surface model. *Cryosphere*, 10, 853–877. doi:10.5194/tc-10-853-2016

Fujii, M., Takano, Y., Kojima, H., Hoshino, T., Tanaka, R., & Fukui, M. (2010), Microbial community structure, pigment composition, and nitrogen source of red snow in Antarctica. *Microb. Ecol.*, 59:466–75. doi:10.1007/s00248-009-9594-9

Fujita, K. (2008), Effect of precipitation seasonality on climatic sensitivity of glacier mass balance. *Earth Planet. Sc. Lett.*, 276, 14–19. doi:10.1016/j.epsl.2008.08.028

Fujita, K., & Ageta, Y. (2000), Effect of summer accumulation on glacier mass balance on the Tibetan Plateau revealed by mass-balance model. *J. Glaciol.*, 46 (150), 244–252. doi:10.3189/172756500781832945

Ganey, G. Q., Loso, M. G., Burgess, A. B., & Dial, R. J. (2017), The role of microbes in snowmelt and radiative forcing on an Alaskan icefield. *Nature Geoscience*. doi:10.1038/NGEO3027

Gorton, H. L., & Vogelmann, T. C. (2003), Ultraviolet radiation and the snow alga Chlamydomonas nivalis (Bauer) Wille. *Photochem. Photobiol*, 77:608–15.

Gray, A., Krolikowski, M., Fretwell, P., Convey, P., Peck, L. S., Mendelova, M., Smith, A. G., & Davey, M. P. (2020), Remote sensing reveals Antarctic green snow algae as important terrestrial carbon sink, *Nat. Commun.*, 11, 2527. doi:10.1038/s41467-020-16018-w

Harris, I. C. (2019), CRU JRA v2.0: A forcings dataset of gridded land surface blend of Climatic Research Unit (CRU) and Japanese reanalysis (JRA) data. Centre for Environmental Data Analysis, https://catalogue.ceda.ac.uk/uuid/7f785c0e80aa4df2b39d068ce7351bbb.

Hisakawa, N., Quistad, S. D., Hestler, E. R., Martynova, D., Maughan, H., Sala, E., Gavrilo, M. V., & Rowher, F. (2015), Metagenomic and satellite analyses of red snow in the Russian Arctic. *Peer J*, 3, e1491. doi:10.7717/peerj.1491

Hodson, A. J., Nowak, A., Cook, J., Sabacka, M., Wharfe, E. S., Pearce, D. A., Convey, P., & Vieira, G. (2017), Microbes influence the biogeochemical and optical properties of maritime Anatarctic snow. *J. Geophys. Res. Biogeosci.*, 122, 1456–70. doi:10.1002/2016JG003694

747 Hoham, R. W., Frey, F. M., Berman, J. D., Ryba, J. B., Duncan, J. E., Forbes, A. A., Goodridge,
748 B. M., & Miller, P. R. (2009), The effects of irradiance level, photoperiod, and cell density on
749 sexual reproduction in the green snow alga, Chloromonas chenangoensis (Chlorophyta,
750 Volvocales), from Upstate New York. *Nova. Hedwigia*, 89:1–16.
751
752 Hoham, R. W., Marcarelli, A. M., Rogers, H. S., Ragan, M. D., Petre, B. M., Ungerer, M. D.,
753 Barnes, J. M., & Francis, D. O. (2000), The importance of light and photoperiod in sexual
754 reproduction and geographical distribution in the green snow alga, Chloromonas sp.-D
755 (Chlorophyseae, Volvocales). *Hydrol. Process*, 14:3309–21.
756
757 Hoham, R. W., & Remias, D. (2020), SNOW AND GLACIAL ALGAE: A REVIEW. *J. Phycol.*,
758 12952. doi:10.1111/jpy.12952
759
760 Huovinen, P., Ramírez, J., & Gómez, I. (2018), Remote sensing of albedo-reducing snow algae
761 and impurities in the Maritime Antarctica. *ISPRS J. Photogramm, Remote Sens.*, 146, 507-517.
762 doi:10.1016/j.isprsjprs.2018.10.01510
763
764 Khan, A. L., Dierssen, H., Scambos, T., Höfer, J., & Cordero, R. R. (2021), Spectral
765 characterization, radiative forcing and pigment content of coastal Antarctic snow algae:
766 approaches to spectrally discriminate red and green communities and their impact on snowmelt.
767 *Cryosphere*, 15, 133–148. doi:10.5194/tc-15-133-2021
768
769 Kim, H. (2017), Global Soil Wetness Project Phase 3 Atmospheric Boundary Conditions
770 (Experiment 1) [Data set], Data Integration and Analysis System (DIAS).
771 doi:10.20783/DIAS.501.
772
773 Krinner, G., Derksen, C., Essery, R., Flanner, M., Hagemann, S., Clark, M., Hall, A., Rott, H.,
774 Brutel-Vuilmet, C., Kim, H., Ménard, C. B., Mudryk, L., Thackeray, C., Wang, L., Arduini, G.,
775 Balsamo, G., Bartlett, P., Boike, J., Boone, A., Chéruy, F., Colin, J., Cuntz, M., Dai, Y.,
776 Decharme, B., Derry, J., Ducharne, A., Dutra, E., Fang, X., Fierz, C., Ghattas, J., Gusev, Y.,
777 Haverd, V., Kontu, A., Lafaysse, M., Law, R., Lawrence, D., Li, W., Marke, T., Marks, D.,
778 Ménégoz, M., Nasonova, O., Nitta, T., Niwano, M., Pomeroy, J., Raleigh, M. S., Schaedler, G.,
779 Semenov, V., Smirnova, T. G., Stacke, T., Strasser, U., Svenson, S., Turkov, D., Wang, T.,
780 Wever, N., Yuan, H., Zhou, W., & Zhu, D. (2018), ESM-SnowMIP: assessing snow models and
781 quantifying snow-related climate feedbacks, *Geosci. Model Dev.*, 11, 5027–5049,
782 doi:10.5194/gmd-11-5027-2018.
783
784 Krinner, G., Viovy, N., de Noblet-Ducoudré, N., Ogée, J., Polcher, J., Friedlingstein, P., Ciais,
785 P., Sitch, S., & Prentice, IC. (2005), A dynamic global vegetation model for studies of the
786 coupled atmosphere-biosphere system, *Global Biogeochem. Cycles*, 19(1), GB1015.
787 doi:10.1029/2003GB002199.
788
789 Lawrence, D. M., Fisher, R. A., Koven, C. D., Oleson, K. W., Swenson, S. C., Bonan, G., et al.
790 (2019), The Community Land Model version 5: Description of new features, benchmarking, and
791 impact of forcing uncertainty. *Journal of Advances in Modeling Earth Systems*.
792 doi:10.1029/2018MS001583

Leya, T., Rahn, A., Lütz, C., & Remias, D. (2009), Response of arctic snow and permafrost algae to high light and nitrogen stress by changes in pigment composition and applied aspects for biotechnology. *FEMS Microbiol. Ecol.*, 67, 432-443. doi:10. 1111/j. 1574-6941.2008.00641.x

Lutz, S., Anesio, A. M., Jorge Villar, S. E., & Benning, L. G. (2014), Variations of algal communities cause darkening of a Greenland glacier. *FEMS Microbiol. Ecol.*, 89, 402–414. doi:10.1111/1574-6941.12351

Lutz, S., Anesio, A. M., Field, K., & Benning, L. G. (2015), Integrated 'omics', targeted metabolite and single-cell analyses of Arctic snow algae functionality and adaptability. *Front. Microbiol*, 6, 1323. doi:10.3389/fmicb.2015.01323

Lutz, S., Anesio, A. M., Raiswell, R., Edwards, A., Newton, R. J., Gill, F., & Benning, L. G. (2016), The biogeography of red snow microbiomes and their role in melting arctic glaciers. *Nature Communications*, doi:10.1038/ncomms11968

Mauro, B. D., Baccolo, G., Garzonio, R., Giardino, C., Massabo, D., Piazzalunga, A., Rossini, M., & Colombo, R. (2017), Impact of impurities and cryoconite on the optical properties of the Morteratsch Glacier (Swiss Alps). *Cryosphere*, 11 (6), 2393-2409. doi:10.5194/tc-11-2393-2017

Moestrup, Ø., Nicholls, K. H., & Daugbjerg, N. (2018), Studies on woloszynskioid dinoflagellates IX: ultrastructure, cyst formation and phylogeny of the 'red-snow' alga Borghiella pascheri (Suchlandt) Moestrup (= Glenodinium pascheri, Woloszynskia pascheri, Gyrodinium nivalis). *Eur. J. Phycol.*, 53, 393–409

Müller, T., Leya, T., & Fuhr, G. (2001), Persistent snow algal fields in Spitsbergen: field observations and a hypothesis about the annual cell circulation. *Arct. Antarct. Alp. Res.*, 33, 42-51. doi:10.2307/1552276

Nagatsuka, N., Takeuchi, N., Nakano, T., Shin, K., & Kokado, E. (2014), Geographical variationsin Sr and Nd isotopic ratios of cryoconite on Asian glaciers. *Environ. Res. Lett.*, 9, 045007, doi:10.1088/1748-9326/9/4/045007

Navarro, F.J., Jonsell U.Y., Corcuera M.I., & Martín-Español A. (2013), Decelerated mass loss of Hurd and Johnsons Glaciers, Livingston Island, Antarctic Peninsula. *J. Glaciol.*, 59(213), 115–128.

Nitta, T., Yoshimura, K., & Abe-Ouchi, A. (2017), Impact of arctic wetlands on the climate system: Model sensitivity simulations with the MIROC5 AGCM and a snow-fed wetland scheme, *J. Hydrometeorol.*, 18, 2923–2936

Nitta, T., Yoshimura, K., Takata, K., O'ishi, R., Sueyoshi, T., Kanae, S., Oki, T., Abe-Ouchi, A., & Liston, G. E. (2014), Representing variability in subgrid snow cover and snow depth in a global land model, *J. Climate*, 27, 3318–3330. doi:10.1175/JCLID-13-003

Novis, P. M. (2002), Ecology of the snow alga Chlainomonas kolii (Chlamydomonadales, Chlorophyta) in New Zealand. *Phycologia*, 41 (3), 280–292. doi:10.2216/i0031-8884-41-3-280.1

Osada, K., Ida, H., Kido, M., & Matsunaga, K. (2004), Iwasaka, Y.: Mineral dust layers in snow at Mount Tateyama, Central Japan: formation processes and characteristics. *Tellus*, 56B, 382-392. doi:10.3402/tellusb.v56i4.16436

Onuma, Y., Yoshimura, K., & Takeuchi., N. (2021). Data set regarding snow algal modeling (Version v1.2) [Data set]. Zenodo. doi:10.5281/zenodo.4626347

Onuma, Y., Takeuchi, N., & Takeuchi, Y. (2016), Temporal changes in snow algal abundance on surface snow in Tohkamachi, Japan. *Bull. Glaciol. Res.*, 34, 21-31. doi:10.5331/bgr.16A02

Onuma, Y., Takeuchi, N., Tanaka, S., Nagatsuka, N., Niwano, M., & Aoki, T. (2018), Observations and modelling of algal growth on a snowpack in north-western Greenland. *Cryosphere*, 12, 2147–2158. doi:10.5194/tc-12-2147-2018

Onuma, Y., Takeuchi, N., Tanaka, S., Nagatsuka, N., Niwano, M., & Aoki, T. (2020), Physically based model of the contribution of red snow algal cells to temporal changes in albedo in northwest Greenland. *Cryosphere*, 14, 2087-2101. doi:10. 5194/tc-14-2087-2020

Painter, T. H., Duval, B., & Thomas, W. H. (2001), Detection and quantification of snow algae with an airborne imaging spectrometer. *Appl. Environ. Microbiol.*, 67, 5267–5272. doi:10.1128/AEM.67.11.5267-5272.2001

Procházková, L., Leya, T., Křížková, H., & Nedbalová, L. (2019), Sanguina nivaloides and Sanguina aurantia gen. et spp. nov. (Chlorophyta): the taxonomy, phylogeny, biogeography and ecology of two newly recognised algae causing red and orange snow. *FEMS Microbiol. Ecol.*, 95:fiz064, doi:10.1093/femsec/fiz064

Remias, D. (2012), Cell structure and physiology of alpine snow and ice algae, in: Plants in alpine regions, Cell physiology of adaption and survival strategies. edited by: Lütz, C., *Springer Wien*, 202, 175–186. doi:10.1007/978-3-7091-0136-0_13.

Remias, D., Albert, A., & Lütz, C. (2010), Effects of realistically simulated, elevated UV irradiation on photosynthesis and pigment composition of the alpine snow alga Chlamydomonas nivalis and the arctic soil alga Tetracystis sp. (Chlorophyceae), *Photosynthetica*, 48, 269–277.

Remias, D., Pichrtová, M., Pangratz, M., Lütz, C., & Holzinger, A. (2016), Ecophysiology, secondary pigments and ultrastructure of Chlainomonas sp. (Chlorophyta) from the European Alps compared with Chlamydomonas nivalis forming red snow, FEMS Microbiol. Ecol., 92:fiw030. doi:10.1093/femsec/fiw030

Sakai, A., & Fujita, K. (2017), Contrasting glacier responses to recent climate change in highmountain Asia. *Sci. Rep.*, 7: 13717. doi:10.1038/s41598-017-14256-5

Segawa, T., Matsuzaki, R., Takeuchi, N., Akiyoshi, A., Navarro, F., Sugiyama, S., Yonezawa, T., & Mori, H. (2018), Bipolar dispersal of red-snow algae. *Nat. Commun.*, 9:3094. doi:10.1038/s41467-018-05521-w

Segawa, T., Miyamoto, K., Ushida, K., Agata, K., Okada, N., & Kohshima, S. (2005), Seasonal Change in Bacterial Flora and Biomass in Mountain Snow from the Tateyama Mountains, Japan, Analyzed by 16S rRNA Gene Sequencing and Real-Time PCR. *App. Environ. Microbiol.*, 71 (1), 123–130. doi:10.1128/AEM.71.1.123–130

Spijkerman, E., Wacker, A., Weithoff, G., & Leya, T. (2012), Elemental and fatty acid composition of snow algae in arctic habitats. *Front. Microbiol.*, 3:380.

Stibal, M., Elster, J., Ŝabacká, M. and Kaŝtovská, K. (2007), Seasonal and diel changes in photosynthetic activity of the snow alga Chlamydomonas nivalis (Chlorophyceae) from Svalbard determined by pulse amplitude modulation fluorometry. *FEMS. Microbiol. Ecol.*, 59, 265–273. doi:10.1111/j.1574-6941.2006.00264.x

Sugiyama, S., Navarro, F. J., Sawagaki, T., Minowa, M., Segawa, T., Onuma, Y., Otero, J., & Vasilenko, E. J. (2019), Subglacial water pressure and ice-speed variations at Johnsons Glacier, Livingston Island, Antarctic Peninsula. *J. Glaciol.*, 65(252), 689–699. doi:10.1017/jog.2019.45

Takata, K., Emori, S., & Watanabe, T. (2003), Development of the Minimal Advanced Treatments of Surface Interraction and RunOff (MATSIRO). *Global Planet. Change*, 38, 209–222.

Takeuchi, N. (2013), Seasonal and altitudinal variations in snow algal communities on an Alaskan glacier (Gulkana glacier in the Alaska range). *Environ. Res. Lett.*, 8, 035002. doi:10.1088/1748-9326/8/3/035002

Takeuchi, N., & Kohshima, S. (2004), snow algal community on a Patagonian glacier, Tyndall glacier in the Southern Patagonia Icefield. *Arct. Antarct. Alp. Res.*, 36, 91–8.

Takeuchi, N., Uetake, J., Fujita, K., Aizen, V. B., & Nikitin, S. D. (2006a), A snow algal community on Akkem Glacier in the Russian Altai Mountains. *Ann. Glaciol.*, 43, 378–84.

Takeuchi, N., Dial, R., Kohshima, S., Segawa, T., & Uetake, J. (2006b), Spatial distribution and abundance of red snow algae on the Harding Icefield, Alaska derived from a satellite image. *Geophys. Res. Lett.*, 33, L21502. doi:10.1029/2006GL027819

Tanaka, S. (2016), Seasonal and inter-annual variabilities of snow and ice algal community on glaciers in the Asia and Arctic regions. *Graduate School of Science, Chiba Univ., Doctoral thesis*.

Tanaka, S., Takeuchi, N., Miyairi, M., Fujisawa, Y., Kadota, T., Shirakawa, T., Kusaka, R., Takahashi, S., Enomoto, H., Ohata, T., Yabuki, H., Konya, K., Fedorov, A., Konstantinov, P.

(2016), Snow algal communities on glaciers in the Suntar-Khayata Mountain Range in eastern Siberia. *Russia. Polar Sci.*, 10, 3, 227-238, doi:10.1016/j.polar.2016.03.004.

Tatebe, H., Ogura, T., Nitta, T., Komuro, Y., Ogochi, K., Takemura, T., Sudo, K., Sekiguchi, M., Abe, M., Saito, F., Chikira, M., Watanabe, S., Mori, M., Hirota, N., Kawatani, Y., Mochizuki, T., Yoshimura, K., Takata, K., O'ishi, R., Yamazaki, D., Suzuki, T., Kurogi, M., Kataoka, T., Watanabe, M., & Kimoto, M. (2019), Description and basic evaluation of simulated mean state, internal variability, and climate sensitivity in MIROC6. *Geosci Model Dev.*, 12, 2727–2765. doi:10.5194/gmd-12-2727-2019

Thomas, W. H., & Duval, B. (1995), Sierra Nevada, California, USA, snow algae: snow albedo changes, algal-bacterial interrelationships, and ultraviolet radiation effects. *Arct. Alp. Res.*, 27, 389–99.

van den Hurk, B., Kim, H., Krinner, G., Seneviratne, S. I., Derksen, C., Oki, T., Douville, H., Colin, J., Ducharne, A., Cheruy, F., Viovy, N., Puma, M. J., Wada, Y., Li, W., Jia, B., Alessandri, A., Lawrence, D. M., Weedon, G. P., Ellis, R., Hagemann, S., Mao, J., Flanner, M. G., Zampieri, M., Materia, S., Law, R. M., & Sheffield, J. (2016), LS3MIP (v1.0) contribution to CMIP6: the Land Surface, Snow and Soil moisture Model Intercomparison Project – aims, setup and expected outcome. *Geosci. Model Dev.*, 9, 2809–2832. doi:10.5194/gmd-9-2809-2016

Vimercati, L., Solon, A. J., Krinsky, A., Arán, P., Porazinska, D. L., & Darcy, J. L. (2019), Nieves penitentes are a new habitat for snow algae in one of the most extreme high-elevation environments on Earth. *Arct. Antarct. Alp. Res.*, 51:1, 190-200. doi:10.1080/15230430.2019.1618115

Weedon, G. P., Balsamo, G., Bellouin, N., Gomes, S., Best, M. J., & Viterbo, P. (2014), The WFDEI meteorological forcing data set: WATCH Forcing Data methodology applied to ERA Interim reanalysis data. *Water Resour. Res.*, 50, 7505–7514. doi:10.1002/2014WR015638

Yoshimura, K., Miyazaki, S., Kanae, S., & Oki, T. (2006), Iso-MATSIRO, a land surface model that incorporates stable water isotopes. *Global Planet. Change*, 51, 90–107. doi:10.1016/j.gloplacha.2005.12.007

Zawierucha, K., & Shain, D. H. (2019), Disappearing Kilimanjaro snow—Are we the last generation to explore equatorial glacier biodiversity? *Ecol. Evol.*, 9, 8911–8918.